electronics

MDPI

Article

Analysis of the ESD Reconstruction Methodology Based on Current Probe Measurements and Frequency Response Compensation for Different ESD Generators and Severity Test Levels

Panagiotis K. Papastamatis, Evangelos A. Paliatsos, Ioannis F. Gonos * and Ioannis A. Stathopulos

High Voltage Laboratory, School of Electrical and Computer Engineering, National Technical University of Athens, 157 80 Athens, Greece; ppapastamatis@central.ntua.gr (P.K.P.); paliatsosevangelos@gmail.com (E.A.P.); stathop@power.ece.ntua.gr (I.A.S.)

* Correspondence: igonos@cs.ntua.gr; Tel.: +30-210-772-3539

Abstract: System-level electrostatic discharge testing according to IEC 61000-4-2 has been the main standardized electrostatic discharge immunity testing procedure for the last few decades. The correlation between a failed test result and the injected electrostatic discharge current waveform characteristics, as well as the reduced reproducibility of the standard methodology, have always concerned product manufacturers and test engineers. In an effort to accurately reconstruct the electrostatic discharge current during immunity testing, researchers are focusing more and more on the usability of current probes in capturing the injected current in "real time". In this article, the results of a proposed methodology, based on current probe measurements and a frequency response compensation method, published in recent bibliography, for different test levels and electrostatic discharge generators are presented, aiming to highlight the advantages and disadvantages of the method, investigate its universal applicability, and introduce points of future work toward the current reconstruction during system-level electrostatic discharge testing effort.

Keywords: current monitor probes; ESD current reconstruction; ESD current recording; frequency response compensation method; IEC 61000-4-2; probe bandwidth; probe loading effect; various test levels and ESD generators

Citation: Papastamatis, P.K.; Paliatsos, E.A.; Gonos, I.F.; Stathopulos, I.A. Analysis of the ESD Reconstruction Methodology Based on Current Probe Measurements and Frequency Response Compensation for Different ESD Generators and Severity Test Levels. *Electronics* **2021**, *10*, 728. https://doi.org/10.3390/electronics10060728

Academic Editor: Paolo Stefano Crovetti

Received: 18 February 2021
Accepted: 17 March 2021
Published: 19 March 2021

1. Introduction

Electrostatic discharges (ESD), together with lightning occurrences, are the most frequently encountered transient events in nature. With charging voltages reaching tens of kV and discharge times of less than 1 ns, electrostatic discharges have been a significant source of not only electromagnetic interference but also physical damage for modern electronics. As technology progresses rapidly and technologies of higher working frequencies are implemented, ESD becomes even more relevant, mainly due to its high frequency characteristics. Sub-ns rise time discharges result in radiated fields and induced disturbances with significant spectrum component at frequencies above 1 GHz, making circuit operating at these frequencies greatly susceptible to potential damage or performance degradation.

Testing against these phenomena has always been a major concern for manufacturers and product designers, leading to a significant amount of research and standardization effort on the accurate and reproducible simulation of ESD events. This effort led to the implementation of two different types of immunity testing to electrostatic discharges: (a) the component-level ESD testing, where specific components are subjected to ESD pulses to evaluate their voltage threshold, and (b) the system-level immunity testing, where the final product, in its normal operation condition, is evaluated regarding a potential performance degradation according to specific, product dependent, Pass/Fail performance criteria.

Component-level testing is based on three different ESD models and conducted according to their associated Standards issued by the ESD Association:

- The Human Body Model or HBM, simulating discharges occurring between a human hand or finger and a conductor. The associated Standard is ANSI/ESDA-JEDEC JS-001-2010 [1].
- The Charged Device Model or CDM, simulating discharges when the device under test becomes charged and discharges to a grounded conductor. The associated Standard is ESD STM5.3.1-2009 [2].
- The Machine Model or MM, simulating discharges from the machine through a device to ground. The associated Standard is ANSI/ESD STM5.2-2012 [3]. Testing according to this model is rapidly getting discontinued across the industry.

System-level ESD testing requires the device to be tested in its normal configuration and the ESD current to be injected to the device either by contact discharges to its accessible conductive surfaces or by air discharges to its insulative components. The main reference standard that describes the characteristics of the injected ESD current, as well as the testing configuration, is the IEC 61000-4-2 Standard [4]. The ESD current waveform and the associated current parameters are presented in Figure 1 [4] and Table 1 [4] and are defined as:

- I_{max}: the maximum current value of the ESD waveform
- T_{rise}: the rising time between the time the current reaches 10% of the I_{max} and the time it reaches 90% of I_{max}
- I_{30ns} and I_{60ns}: the current value at the 30 ns and 60 ns time points measured from the time point the current reaches 10% of I_{max} for the first time

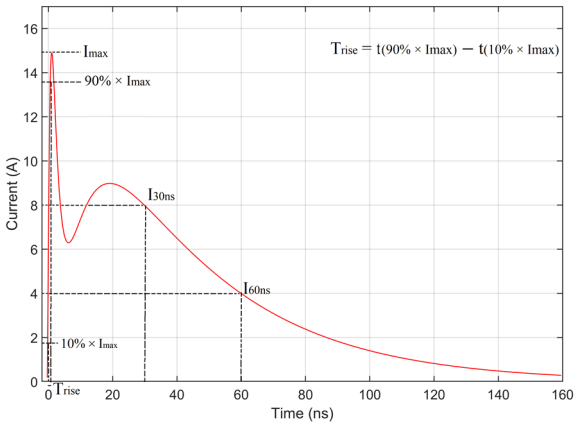

Figure 1. 4 kV electrostatic discharges (ESD) current waveform according to IEC 61000-4-2.

Table 1. ESD parameters according to IEC 61000-4-2.

Level	Charging Voltage	I_{max}	T_{rise}	I_{30ns}	I_{60ns}
	(kV)	(A)	(ns)	(A)	(A)
1	2	7.5	0.8	4	2
2	4	15	0.8	8	4
3	6	22.5	0.8	12	6
4	8	30	0.8	16	8

Figure 2 [4] presents the testing configuration according to IEC 61000-4-2 [4] for table-top equipment. All waveforms presented in this work are extracted from the Matlab software.

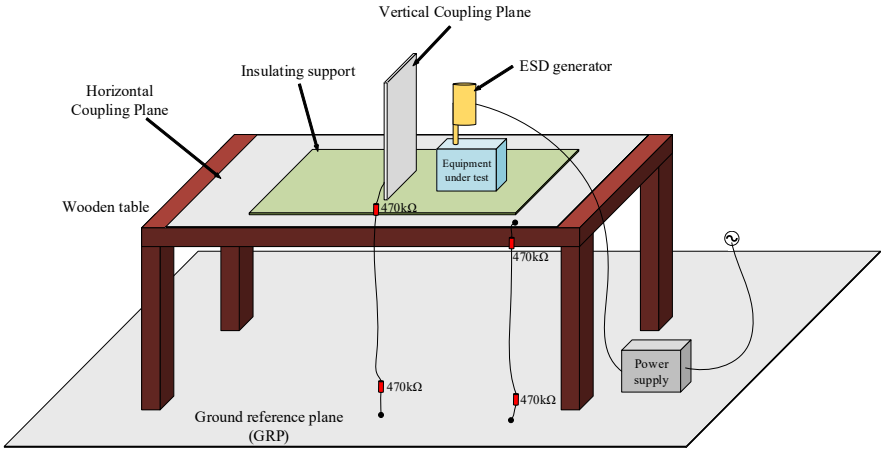

Figure 2. ESD testing configuration according to IEC 61000-4-2.

As for every standardized test method, the repeatability and reproducibility of the applied methodology play a significant role regarding the methodology validity. Unfortunately, the IEC 61000-4-2 [4] has not displayed satisfying results for these parameters, especially regarding the Pass or Fail result of an ESD immunity test. This conclusion resulted from a Round Robin (RR) test, which was carried out in the USA and Japan in 2006. The observations, regarding the limited repeatability and reproducibility of the IEC 61000-4-2 [4] method, are presented in more detail in ref. [5] and ref. [6]. In order to better investigate these limitations and provide product manufacturers and designers with improved troubleshooting tools, researchers are focusing more and more on the real-time recording of the ESD waveform injected to the device under test during system-level ESD testing. Calculation of the critical values of the maximum current (I_{max}), the rise time of the initial peak (T_{rise}), the current at 30 ns (I_{30ns}) and 60 ns (I_{60ns}), as defined in IEC 61000-4-2 [4] and presented in Table 1, as well as the transferred charge during testing, may significantly contribute to determining the causes of a "Fail" result. The ability to attribute a specific product failure either to the higher frequency component of the ESD current, which is associated with the I_{max} and T_{rise} parameters or to the lower frequency component, which is associated with the I_{30ns}, I_{60ns}, and transferred charge parameters can significantly improve the troubleshooting procedure. Additionally, the collection of a satisfyingly large amount of testing data and the necessary correlation between failures and current parameters can potentially lead to the adjustment of the tolerance limits for those parameters by the standardization committees to better suit the repeatability and reproducibility requirements. The results of the aforementioned RR test [5,6] clearly indicate that the ESD current parameters may vary significantly and still be within the tolerance limits defined in IEC 61000-4-2 [4].

Therefore, real-time recording can be a very useful tool not only for better defining those tolerance limits but also potentially for bringing new parameters to the foreground correlated to the Pass or Fail result of a system-level ESD test. Its methodology is based on the ESD current reconstruction, which has drawn the attention of researchers in the last few years [7,8] utilizing (a) measurements with a current probe and (b) a frequency response compensation method presented in ref. [8]. In this article, an investigation of the current reconstruction methodology for four different positive test levels (from +2 kV to +8 kV) and four different commercially available ESD test generators is presented. This article aims at better highlighting the strengths/weaknesses of the method, as well as some key points regarding its effectiveness and universal applicability. It also provides specific values for the optimization of the method parameters for each test level and ESD generator, increasing the usability of the method by different laboratories and for different types of test equipment.

2. Frequency Response Compensation Method

Current probes have assisted Electromagnetic Compatibility (EMC) engineers over the last decades in monitoring common-mode currents and troubleshooting EMC problems. Extended uses of these probes were presented in detail in ref. [9]. Another very important application of measurements via current probes has been presented in ref. [8], describing the usage of these probes in collaboration with a relatively simple frequency compensation method in order to reconstruct the ESD current waveform during system-level ESD testing according to IEC 61000-4-2 [4]. This article, utilizing this methodology, aims at presenting details regarding its applicability and to present results for different test levels and ESD test generators. The methodology described in this article consists of three sections: (a) measurements of ESD currents with a current probe and a current target (Pellegrini target), as defined in the calibration process of IEC 61000-4-2 [4], (b) the deconvolution procedure, performed in the frequency domain with the Matlab software and (c) the optimization of the detrend values. The methodology is summarized in the flowchart of Figure 3.

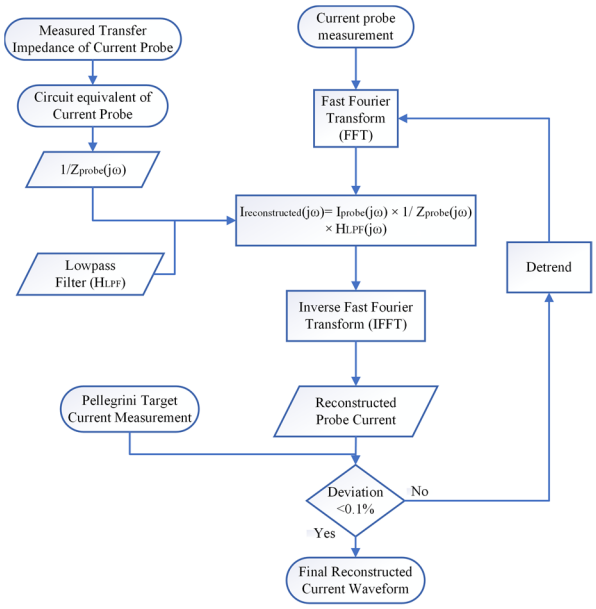

Figure 3. Flowchart of the frequency response compensation method including the detrend optimization process.

2.1. Measurement Equipment and Setup

The experimental procedure complies with the calibration requirements of IEC 61000-4-2 [4], which defines the characteristics of the 2Ω current target used to discharge the ESD current, as well as the required test setup (positioning of the ESD generator, cable routing etc.). The measurement setup, including the ESD generator, the current probe, the Pellegrini target, the oscilloscope inside a Faraday cage, as well as the necessary attenuators for the protection of the oscilloscope, is presented in Figure 4. The current target used for the measurements is the MD 103 Pellegrini Target by Teseq [10]. A very important factor regarding ESD measurements is the bandwidth of the measuring equipment. IEC 61000-4-2 [4] requires an oscilloscope with bandwidth greater than 2 GHz to be used. However, the research presented in ref. [11] points out that the necessary bandwidth to correctly record ESD waveforms and minimize the associated measurement uncertainty is significantly greater. The chosen oscilloscope for the measurements is the TDS 7254B oscilloscope by Tektronix [12] with a bandwidth of 2.5 GHz and a sampling rate of 20 GS/s. As shown in Figure 4, a current probe is mounted around the tip of the ESD generator to record the ESD current waveform injected into the Pellegrini target. Currently, there is a variety of current probes commercially available, which are suitable for ESD measurements. Tektronix has released the CT series [13], which offers bandwidth capabilities up to 2 GHz. However,

these probes are designed to be mounted around very small conductors and are therefore not suitable to be mounted around the ESD generator tip. Fortunately, Fischer Custom Communications produces probes of larger inner diameter—with reduced bandwidth capabilities (1 GHz)—such as the one used for the measurements in this study. The probe used is the FCC F-65 Current Monitor Probe [14]. The recording time window is set between −4 and 156 ns, capturing the entirety of the ESD waveform, allowing the estimation of the total charge injected from the ESD generator to the current target. The 40 ps value was the chosen time step and the number of recorded values was 4000.

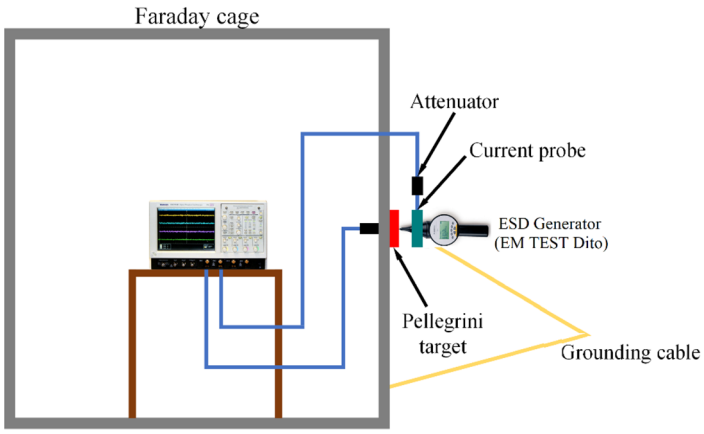

Figure 4. Test setup for measurements of the EM TEST Dito ESD generator via the F-65 current probe and the Pellegrini target.

2.2. Deconvolution Process

Deconvolution is defined as the process of filtering a signal to compensate for an undesired convolution. The undesired convolution in the case of the aforementioned measurement procedure emerges from the low-frequency roll off of the current probe and its limited bandwidth (1 GHz). This distortion can be easily observed when comparing the two acquired waveforms before any compensation method is implemented. The waveform acquired from the Pellegrini target and the initial waveform acquired with the current probe are presented in Figure 5.

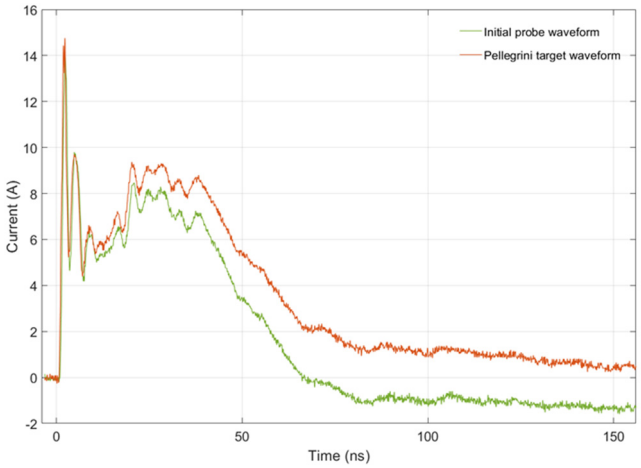

Figure 5. The ESD waveform acquired from the Pellegrini target (orange) and the initial acquired waveform with the current probe without the application of the frequency response compensation method (green).

The deconvolution process is summarized in Equation (1):

$$I_{reconstructed}(j\omega) = I_{probe}(j\omega) \times \frac{1}{Z_{probe}(j\omega)} \times H_{LPF}(j\omega) \quad (1)$$

where

- The $I_{probe}(j\omega)$ factor results from the Fast Fourier Transform of the current waveform acquired with the current probe;
- $Z_{probe}(j\omega)$ can be calculated from the equivalent circuit of the probe calibration procedure, presented in Figure 6 [8], when its transfer impedance magnitude is available from the datasheet [14], usually provided by the manufacturer (Figure 7);

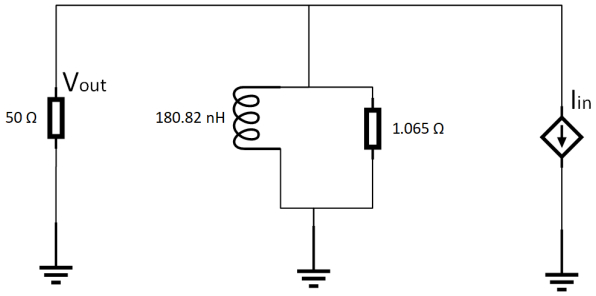

Figure 6. Equivalent circuit of the F-65 current monitor probe calibration procedure.

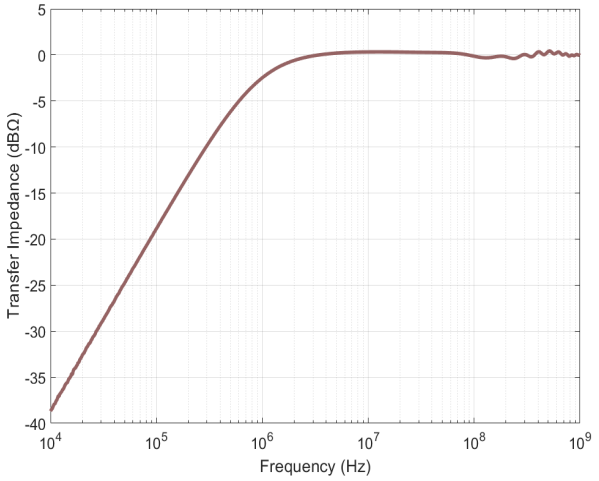

Figure 7. Transfer impedance magnitude of the F-65 current monitor probe.

- The $H_{LPF}(j\omega)$ factor is the transfer function of a low-pass filter with a cut-off frequency equal to the bandwidth of the probe, which is the case of the F-65 probe is 1 GHz, implemented to integrate the bandwidth limitation. The low-pass filter used is a simple first-order RC filter with the transfer function of Equation (2):

$$H_{LPF}(j\omega) = \frac{1}{1 + j\omega C_{LPF} R_{LPF}} \quad (2)$$

The values of C_{LPF} and R_{LPF}, used in Matlab, were selected as 100 Ω and 1.592 pF accordingly for a cut-off frequency of 1 GHz. The vertical transition of the filter was selected as the typical −20 dB/decade slope. The authors decided to use this representation of the filter, which includes the vertical transition, instead of an ideal filter representation (with 100% attenuation above 1 GHz), to better reflect, even qualitatively, the probe behavior above 1 GHz.

The reconstructed ESD current in the time domain can be calculated using the Inverse Fast Fourier Transform of $I_{reconstructed}(j\omega)$.

Here, it should be noted that the circuit of Figure 6 is not the equivalent circuit of the probe, where every parasitic characteristic needs to be simulated, but rather a simplified equivalent circuit of the probe calibration procedure, which is used to match the magnitude diagram of the probe transfer impedance of Figure 7, where the probe is modeled as an inductor. As it is extensively explained in ref. [8], for current probes with a flat region in their transfer impedance diagram, such as the F-65 probe, the realistic probe can be adequately approximated by only the addition of RL elements. Another point that is also discussed in ref. [8] is the requirement of the phase measurements from the calibration report for the circuit modeling procedure. Authors in ref. [8] based on the rather simple structure of current probes, as pure delay terms, consider the equivalent circuit as a minimal phase system. Another assumption made during this process is linearity, which means that the current values are not large enough to cause saturation of the current probe core. The aforementioned assumptions and simplifications are verified by measurement and modelization results in [8] between the modeled probe transfer impedance measurements and real transfer impedance measurements.

2.3. Optimization of the Detrend Values

The DC offset of an oscilloscope is defined as the unwanted DC voltage appearing at the output of the operational amplifier of an oscilloscope overlapping with the desired signal. In general, the DC offset does not distort the initial signal significantly; however, when a current probe is used for measuring ESD currents, the latter part of the acquired waveform is distorted significantly. This distortion is attributed to the integrative nature of the current probe and can be compensated by detrending the initially acquired waveform, which means adding or subtracting a DC value to the entirety of the waveform so that the resulting detrended waveform and the waveform acquired from the Pellegrini target approach zero the same way.

The optimization procedure, as also shown in the flowchart of Figure 3, includes the comparison of the undetrended deconvoluted waveform with the reference waveform acquired with the Pellegrini target. The current values for the last 80 measurement points of the reconstructed, undetrended waveform (Figure 8) are compared with the reference waveform, and their deviation is calculated. If this deviation exceeds the 0.1% value, the detrend value applied to the initial waveform acquired with the current probe must be readjusted, and the entire frequency response compensation method must be reimplemented. Figure 9 presents the initial probe current waveform, the reference Pellegrini target waveform, and the final detrended (with a detrend value of 0.87) and deconvoluted (via the aforementioned frequency response compensation method) waveform for a +4 kV pulse.

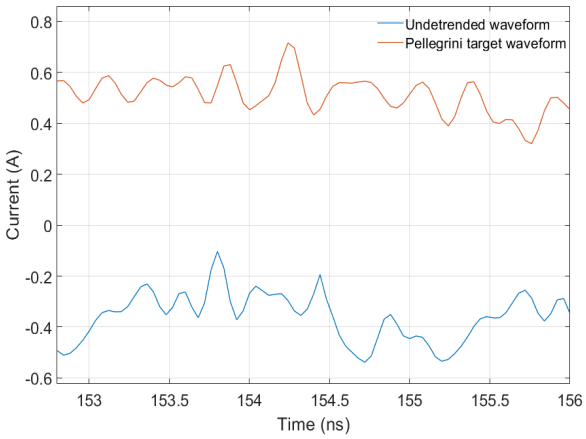

Figure 8. Comparison of the current values of the undetrended waveform with the reference waveform for the last 80 measurement points.

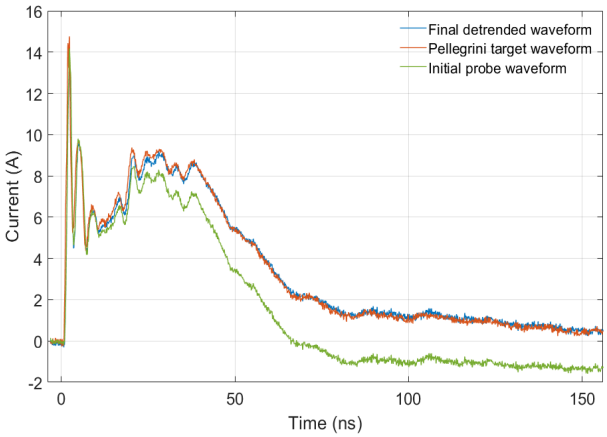

Figure 9. Comparison of the Pellegrini target (reference) waveform, the initial current probe acquired waveform, and the final detrended (reconstructed) waveform for a +4 kV pulse with the EM Test Dito generator.

3. Measurements and Results

The measurements were carried out according to the measurement setup of Figure 2. For each test level and ESD generator, five measurements are performed according to IEC 61000-4-2 [4], in an effort to reduce the repeatability uncertainty of the measurements. The results for the average detrend values, calculated via the frequency response compensation method described in Section 2, for +2 kV, +4 kV, +6 kV, and +8 kV and four commercially available ESD generators (EM Test Dito [15], Schaffner NSG 433 [16], Schaffner NSG 438 [17], and EMC Partner Transient 3000 [18]), as well as the vertical resolution setting of the oscilloscope (Volt/div) are presented in Table 2 [19].

Table 2. Detrend values for different test levels and ESD test generators [19].

Voltage Level (kV)	I_{max} (A)	mV/ div	Detrend Value			
			DITO	NSG 433	NSG 438	Transient 3000
2	7.5	100	0.40	0.45	0.38	0.51
4	15	200	0.88	0.96	0.84	0.95
6	22.5	500	1.17	1.39	1.12	1.28
8	30	500	1.52	1.91	1.50	1.45

Tables 3–6 that follow present the average values over five measurements calculated waveform parameters of the detrended waveform for each test level and ESD generator. Five different parameters are presented: (a) the four current parameters defined in the IEC 61000-4-2 [4] Standard, which are the maximum value of the initial peak (I_{max}), the rise time of the initial peak (T_{rise}), and the current values at 30ns and 60ns (I_{30ns}, I_{60ns}) (b) the transferred charge injected by the generator to the Pellegrini target, calculated as the integral of the entire resulting ESD current waveform. For each test level and ESD generator, two set of measurements are presented: (a) the aforementioned current parameters for the detrended, reconstructed waveform and (b) the corresponding parameters for the reference waveform acquired with the Pellegrini target. The results show a good approximation of most of the parameters by the frequency response compensation for all test levels and ESD generators. The deviation of the I_{max} and T_{rise} parameters observed between the values of the detrended (Current probe) and the reference (Pellegrini) waveforms is attributed to the limited bandwidth of the current monitor probe used and the undesired probe loading effect.

Table 3. Reconstructed and reference ESD current parameters for the EM TEST Dito ESD generator [19].

Voltage Level (kV)		DITO				
		I_{max} (A)	T_{rise} (ns)	I_{30ns} (A)	I_{60ns} (A)	Charge (nC)
2	Probe	7.260	0.927	3.852	1.872	236.226
	Pellegrini	7.581	0.853	4.059	1.839	245.346
4	Probe	13.757	0.961	8.125	3.326	440.175
	Pellegrini	14.760	0.893	8.085	3.291	481.197
6	Probe	21.102	0.928	13.296	5.183	697.017
	Pellegrini	23.100	0.903	13.427	5.166	675.119
8	Probe	28.135	0.934	17.654	6.532	1022.790
	Pellegrini	31.200	0.893	17.813	6.788	952.539

Table 4. Reconstructed and reference ESD current parameters for the Schaffner NSG 433 ESD generator.

Voltage Level (kV)		NSG 433				
		I_{max} (A)	T_{rise} (ns)	I_{30ns} (A)	I_{60ns} (A)	Charge (nC)
2	Probe	7.028	0.843	4.260	2.244	247.505
	Pellegrini	8.261	0.774	4.391	2.196	252.748
4	Probe	13.362	0.876	8.290	4.730	487.831
	Pellegrini	16.12	0.781	8.596	4.828	505.311
6	Probe	20.270	0.886	12.279	7.553	702.640
	Pellegrini	24.570	0.780	12.997	7.394	672.770
8	Probe	26.550	0.878	16.817	9.380	927.514
	Pellegrini	33.000	0.803	16.930	9.811	962.414

Table 5. Reconstructed and reference ESD current parameters the Schaffner NSG 438 ESD generator.

Voltage Level (kV)		NSG 438				
		I_{max} (A)	T_{rise} (ns)	I_{30ns} (A)	I_{60ns} (A)	Charge (nC)
2	Probe	6.845	0.992	3.750	1.826	235.401
	Pellegrini	7.240	0.880	3.812	1.992	210.533
4	Probe	13.448	0.992	7.858	3.929	443.443
	Pellegrini	14.597	0.940	7.999	3.891	445.058
6	Probe	20.300	0.978	11.352	5.327	699.519
	Pellegrini	22.078	0.935	11.632	6.417	750.566
8	Probe	26.871	0.997	15.438	8.366	859.528
	Pellegrini	29.381	0.898	15.570	8.510	920.851

Table 6. Reconstructed and reference ESD current parameters the EMC Partner Transient 3000 ESD generator.

Voltage Level (kV)		Transient 3000				
		I_{max} (A)	T_{rise} (ns)	I_{30ns} (A)	I_{60ns} (A)	Charge (nC)
2	Probe	7.428	0.847	3.426	2.383	192.038
	Pellegrini	7.686	0.804	3.547	2.347	211.415
4	Probe	14.911	0.848	6.593	4.537	396.891
	Pellegrini	15.840	0.819	7.007	4.668	397.391
6	Probe	21.212	0.847	9.689	6.216	546.803
	Pellegrini	22.648	0.822	10.094	6.415	637.437
8	Probe	30.194	0.847	13.624	7.761	805.594
	Pellegrini	32.800	0.829	14.031	7.998	817.362

Figures 10–13 present the waveform of the reconstructed current using the frequency response compensation method and the reference waveform for each ESD generator. The displayed waveforms refer only to one of the five recorded pulses at the +4 kV test level. All waveforms show satisfying convergence, especially for the latter part of the waveform, which is associated with the I_{30ns}, I_{60ns}, and transferred charged parameters. The expected deviation at the initial peak, associated with the I_{max} and T_{rise} parameters, can be observed in the zoomed view complementing each figure. The two waveforms for each ESD generator seem to converge completely after 5–6 ns and for the entirety of the remaining pulse duration.

The results presented in Tables 3–6 clearly demonstrate the strengths and weaknesses of the ESD current reconstruction methodology using probe measurements and the frequency response compensation method. The low-frequency component of the waveform, that includes the I_{30ns}, I_{60ns}, and transferred charge parameters, is approximated by this methodology to a very satisfying extent. This can also be shown by observing the latter part of the waveforms in Figures 10–13. However, as the zoomed views of the initial peak in the same figures show, the methodology does not perform equally satisfyingly in reconstructing the high-frequency component (i.e., I_{max} and T_{rise} parameters). Therefore, it is essential to calculate the percentage deviation for these parameters between the reconstructed and the reference waveforms. These values are calculated according to Equations (3) and (4), and the results are presented in Tables 7 and 8 [19].

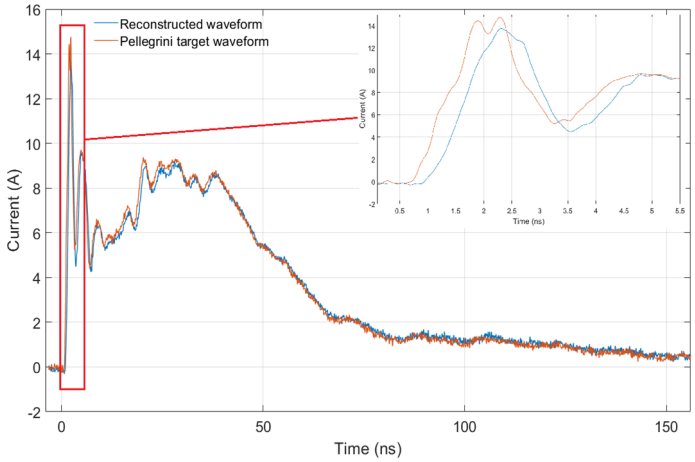

Figure 10. Comparison of the reconstructed waveform applying the proposed methodology with the Pellegrini target (reference) waveform for a +4 kV pulse of the EM TEST Dito ESD generator including a zoomed view of the initial peak.

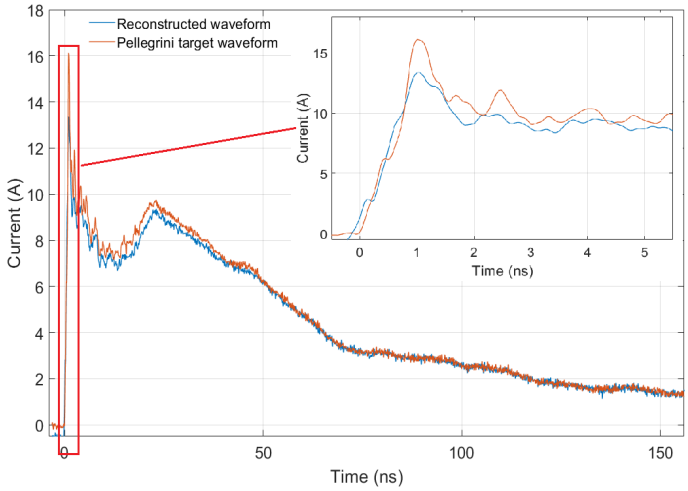

Figure 11. Comparison of the reconstructed waveform applying the proposed methodology with the Pellegrini target (reference) waveform for a +4 kV pulse of the Schaffner NSG 433 ESD generator including a zoomed view of the initial peak.

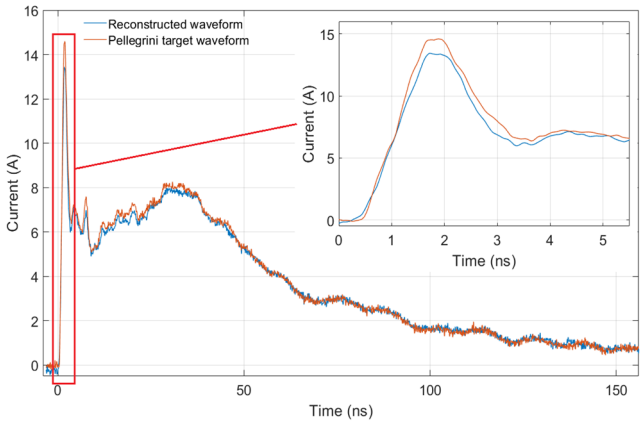

Figure 12. Comparison of the reconstructed waveform applying the proposed methodology with the Pellegrini target (reference) waveform for a +4 kV pulse of the Schaffner NSG 438 ESD generator including a zoomed view of the initial peak.

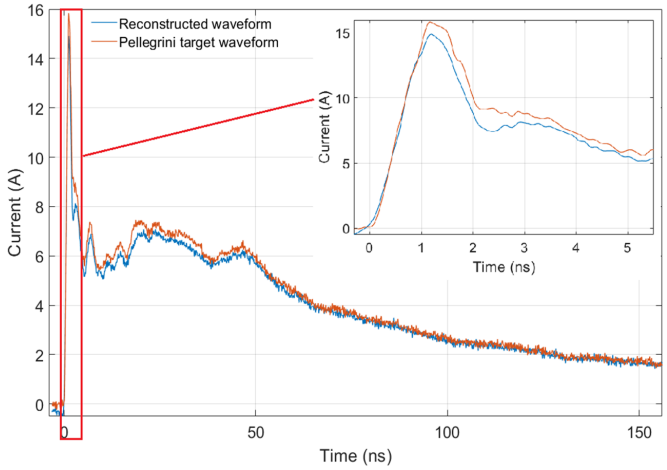

Figure 13. Comparison of the reconstructed waveform applying the proposed methodology with the Pellegrini target (reference) waveform for a +4 kV pulse of the EMC Partner Transient 3000 ESD generator including a zoomed view of the initial peak.

$$I_{max,\ deviation} = \left| \frac{I_{max,Reconstructed} - I_{max,\ Pellegrini}}{I_{max,\ Pellegrini}} \right| \times 100\% \quad (3)$$

$$T_{rise,\ deviation} = \left| \frac{T_{rise,Reconstructed} - T_{rise,\ Pellegrini}}{T_{rise,\ Pellegrini}} \right| \times 100\% \quad (4)$$

where
the $I_{max,Pellegrini}$ and $T_{rise,Pellegrini}$ are the I_{max} and T_{rise} values of the reference waveform acquired with the Pellegrini target and $I_{max,Reconstructed}$ and $T_{rise,Reconstructed}$ are the values calculated for the reconstructed waveform.

Table 7. I_{max} deviation for different test levels and ESD generators [19].

Voltage Level (kV)	mV/div	$I_{max,deviation}$ (%)			
		DITO	NSG 433	NSG 438	Transient 3000
2	100	4.42	17.54	5.77	3.47
4	200	7.29	20.64	8.54	6.23
6	500	9.47	21.21	8.76	6.77
8	500	10.89	24.29	9.34	8.63

Table 8. T_{rise} deviation for different test levels and ESD generators [19].

Voltage Level (kV)	mv/div	$T_{rise,deviation}$ (%)			
		DITO	NSG 433	NSG 438	Transient 3000
2	100	7.98	8.19	11.29	5.08
4	200	7.08	10.84	5.24	3.42
6	500	2.69	11.96	4.40	2.95
8	500	4.39	8.54	9.93	2.13

The results of Table 7 lead to the following observations:

- The I_{max} deviation increases with the increase of the voltage level. This is observed for all four ESD generators studied. More specifically, the +4 kV test level, which is the most commonly used voltage level for contact mode ESD testing according to IEC 61000-4-2 [4], shows deviation values between 6% and almost 21%. It should be noted that the acceptable deviation specified in the IEC 61000-4-2 Standard [4] is 15%. Therefore, there is the possibility for an ESD generator with calibrated ESD current parameters within the tolerance limits of the associated standard to display, during current probe measurements, values for these parameters that are not acceptable according to the standard.
- The I_{max} deviation shows significant variation between the ESD generators tested, reducing the universal applicability of the frequency response compensation method and highlighting the necessity for further investigation prior to using this methodology for a specific ESD generator. The verification procedure is the procedure described in this article, where the current probe measurements are compared to the reference measurements from the Pellegrini target.
- The differences in the compensation method behavior across the four different ESD generators, observed for the initial peak parameters, can be attributed mainly to the limited initial peak compensation capabilities of the proposed methodology due to the limited bandwidth of the measuring probe (1 GHz) not allowing the initial peak to be reconstructed with the proper detail by attenuating the high-frequency component. A secondary factor affecting the reconstruction of the initial peak is the mounting position of the current probe around the tip of each generator. Due to the manufacturing differences in the design of each generator, the current probe mounting

position cannot be reproduced accurately over all four ESD generators, introducing potentially a large uncertainty factor.

The results of Table 8 highlight also the variation of the T_{rise} deviation between different test levels and ESD generators. Here, no pattern can be identified for the different test levels, but the "per case" approach and verification described above is emphasized, observing the deviation between the ESD generators.

Finally, Figures 14–17 present the initial peak of the reconstructed and reference waveforms for all test levels for each of the four ESD generators, graphically displaying the aforementioned deviations.

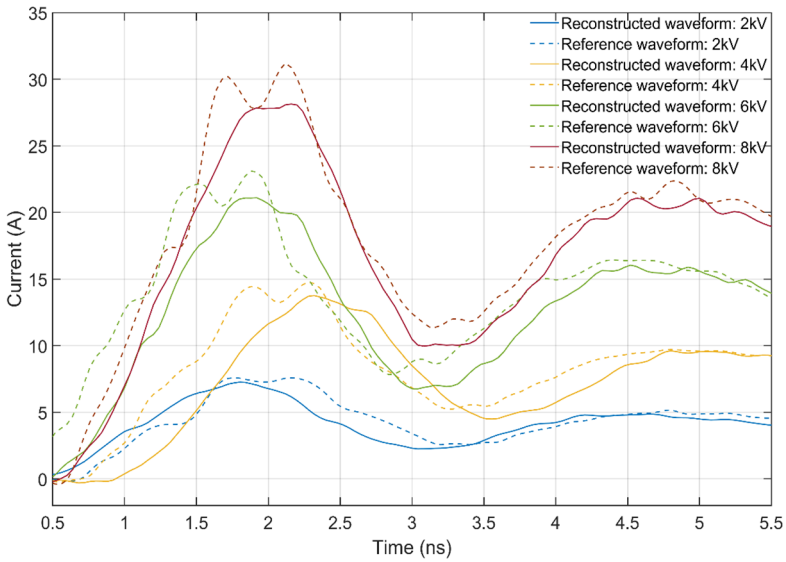

Figure 14. Initial peak comparison of the reconstructed waveform (straight lines) with the Pellegrini target (reference) waveform (dotted lines) for a +2 kV (blue), +4 kV (yellow), +6 kV (green) and +8 kV (red) pulse of the EM Test Dito generator.

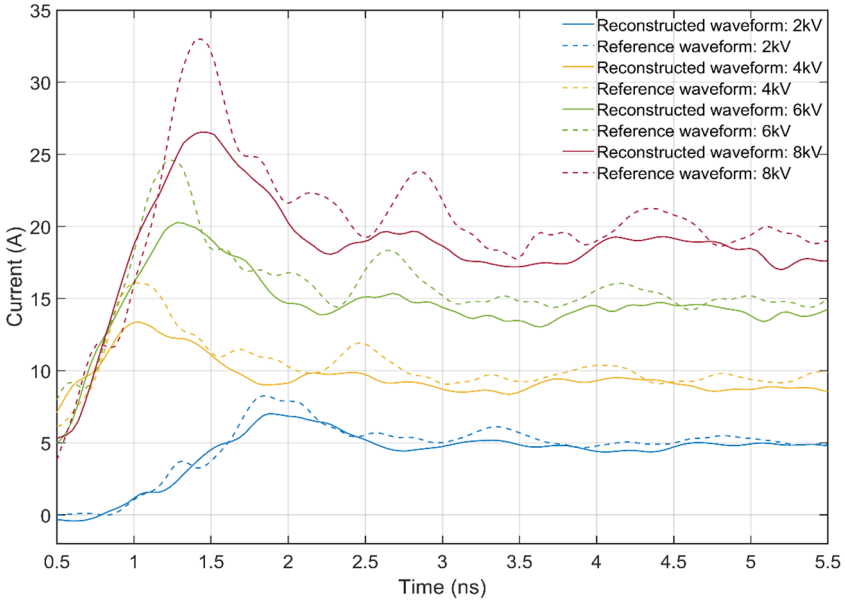

Figure 15. Initial peak comparison of the reconstructed waveform (straight lines) with the Pellegrini target (reference) waveform (dotted lines) for a +2 kV (blue), +4 kV (yellow), +6 kV (green) and +8 kV (red) pulse of the Schaffner NSG 433 generator.

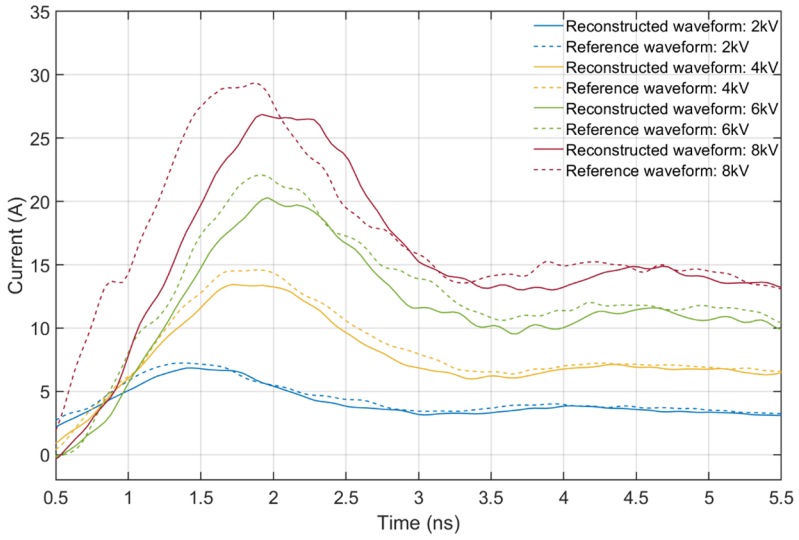

Figure 16. Initial peak comparison of the reconstructed waveform (straight lines) with the Pellegrini target (reference) waveform (dotted lines) for a +2 kV (blue), +4 kV (yellow), +6 kV (green) and +8 kV (red) pulse of the Schaffner NSG 438 generator.

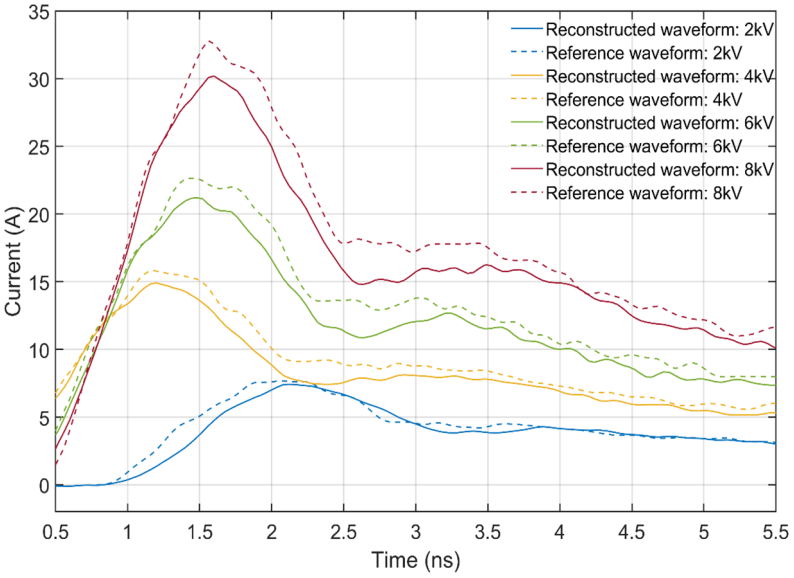

Figure 17. Initial peak comparison of the reconstructed waveform (straight lines) with the Pellegrini target (reference) waveform (dotted lines) for a +2 kV (blue), +4 kV (yellow), +6 kV (green) and +8 kV (red) pulse of the EMC Partner Transient 3000 generator.

4. Discussion

The measurement results, as presented in the previous section, show the adequately accurate reconstruction of the ESD current waveform by the frequency response compensation method based on the measurements acquired with a current probe mounted on the tip of an ESD generator. However, the same results indicate the limitations of this specific method. These limitations and the resulting observations regarding the results at different voltage levels and for different ESD generators are discussed below.

4.1. Detrend Values and Their Applicability

The results of Table 2 clearly show the linearity between the calculated detrend values and the corresponding voltage level. This linear relationship is observed for all ESD generators used during the measurements. The vertical resolution setting of the

oscilloscope does not seem to influence the calculated values, as shown from the values calculated for the +6 kV and +8 kV levels, where the same vertical resolution is used. The detrend values show also relatively small deviation between the different ESD generators increasing the universal applicability and effectiveness of the proposed methodology. Regarding the detrend values, it should be noted that the calculation of the exact values can vary between different implementation parameters during the deconvolution procedure of Section 2. Parameters, such as the sampling frequency used for the Fast Fourier and Inverse Fast Fourier Transforms, which can vary depending on the sampling rate used for the probe transfer impedance data extracted from the calibration data, as well as the exact characteristics of the low-pass filter implemented, simulating the filtering behavior of the current probe for frequencies above its maximum operating frequency, which in the case of the F-65 probe is 1 GHz, can result in different calculated detrend values during the optimization procedure. Nevertheless, it can be safely concluded that the displayed linear correlation is valid for all different ESD generators, regardless of the exact detrend values calculated.

4.2. Limitations Due to the Limited Bandwidth of the Current Probe

The bandwidth is perhaps the most important property regarding the measuring equipment. The very commonly used rule of thumb when choosing the bandwidth of any measuring equipment is for the chosen bandwidth to be at least 5 times greater in respect to the desired signal bandwidth, which in the case of the ESD waveform defined in IEC 61000-4-2 [4] is 0.35/0.8 ns = ~438 MHz. This rule of thumb sets the requirement during ESD measurements for the chosen bandwidth to ~2.2 GHz, explaining also the IEC 61000-4-2 [4] requirement for a >2 GHz oscilloscope bandwidth.

The limited bandwidth (1 GHz) of the F-65 probe is expected to significantly distort signals of higher bandwidth, such as the ones present in the initial peak of an ESD waveform. Apart from the general attenuation of the initial peak, as indicated by the measurement results of Section 3, the reduced bandwidth can potentially lead to faster peaks within the initial peak rise time to not be correctly recorded. This limitation of the proposed methodology is attributed entirely to the limited capabilities of currently commercially available current probes, which cannot simultaneously offer high current capabilities, a large enough diameter for it to be mounted around the ESD generator tip, and increased bandwidth. However, the proposed methodology offers the flexibility for it to be adjusted in the future, which is in accordance with the increased capabilities. This can be achieved by simply adjusting the cut-off frequency of the low-pass filter, which is introduced to remove unwanted frequency components due to the unknown behavior of the probe's frequency response above its operating range, which may also be a function of capacitive and inductive coupling, causing information above this upper frequency limit to be potentially unusable.

The results of Tables 3–8 clearly show the performance of the frequency response compensation method for the two frequency components of any given ESD current waveform. While the low-frequency component of the slow part of the ESD pulse, i.e., the part of the waveform after the initial peak, is approximated with great accuracy, as displayed by the results of the I_{30ns} and I_{60ns} parameters, the high-frequency component of the fast part of the discharge displays significant deviations regarding its reconstruction. The two associated parameters (I_{max} and T_{rise}) display maximum deviation values up to ~24% and ~12% accordingly. Tables 7 and 8 also emphasize that the performance of the method varies for different test levels and ESD generators. Therefore, it can be concluded that the frequency response compensation method cannot be used, without prior investigation, for every commercially available ESD generator.

4.3. Limitations Due to the Probe Loading Effect

Figures 14–17 present the initial peak behavior of the reconstructed ESD current via probe measurements. In addition to the aforementioned limited bandwidth, another dis-

torting factor can be observed, which is the probe loading effect introduced by the current probe, in this case the F-65 probe. RF transformer-type probes insert some impedance to the circuit they are probing, distorting this way the wanted signal in various ways. This distortion includes an undesired amplitude attenuation, an increase to the rise time of the probed signal, and potentially an unwanted phase shift. More on the models for the circuit loading of current probes and the proposed physical models can be found in refs. [20,21].

The experimental setup used for the measurements in this article, as shown in Figure 4, requires for the current probe to be mounted around the tip of the ESD generator. This requirement, in addition to the fact that the initial peak of the ESD pulse is generated from the tip and the body of the ESD generator, result in a significant distortion of the high-frequency component of the reconstructed ESD waveform. In order to avoid the limitations introduced by this effect, researchers are recently focusing more and more on reconstructing the ESD current waveform via measurements using the current probe around the ground strap of the ESD generator [7]. The research results, presented in [20], could potentially be of significant assistance in the effort to simulate the probe loading effect using an EM simulation software, to better understand its characteristics and contribution to the distortion of the initial peak of the reconstructed ESD waveform.

5. Conclusions and Future Work

The current work presents the results for the application of an ESD current reconstruction methodology, based on a frequency response compensation method and measurements with a current probe mounted on the tip of the ESD generator, to be used during system-level ESD testing according to the IEC 61000-4-2 Standard [4] for different voltage test levels and ESD generators. The contribution of this work includes the investigation of the applicability of the proposed methodology (a) for most of the commercially available ESD generators, (b) for every test level specified in the associated standard, and (c) by every laboratory, contributing to the effort toward a parallel to the ESD compliance testing procedure, which can offer manufacturers more insight on the underlying cause of a product failure and improve its repeatability and reproducibility. The obtained outcomes highlight the advantages and disadvantages of the proposed methodology, clearly showing the different degrees of performance for the two different components of the ESD current waveform. Regarding the low-frequency component of the waveform, the methodology displayed consistent performance for all test levels and ESD generators. However, regarding the initial peak reconstruction, the methodology showed significant variations between different ESD generators, especially for the higher voltage test levels (+6 kV and +8 kV), limiting its applicability and requiring prior investigation for every specific ESD generators chosen for the ESD testing. Summarizing, the frequency response compensation method can be a very useful tool for the reconstruction of ESD current waveforms according to IEC 61000-4-2 [4] by implementing a non-invasive measurement procedure, requiring no modifications to the ESD generator or the measurement setup, staying within the testing requirements of the standard. Additionally, by using the probe around the tip of the ESD generator, the entirety of the ESD waveform is captured, and no "information" is lost. Nevertheless, this method introduces limitations, regarding its universal applicability, associated with the limited bandwidth of the current probe and the probe loading effect. As technology progresses rapidly, the bandwidth limitation can be eventually mitigated by the introduction of probes with greater bandwidth; however, the probe loading effect, which is intrinsic to the presented measurement procedure, requires further research and the assistance of EM simulation software.

Future work includes the evaluation of the method for negative polarity ESD pulses, as well as the comparison of the results presented in this article with results acquired with different current probes, in order to better investigate the probe-loading effect on the initial peak measurements. The utilization of an electromagnetic simulation software and the efficient circuit modeling techniques presented in recent bibliography [22–31], for the investigation of the method for a wider frequency range (potentially up to 6 GHz), can

provide useful information regarding the parameters taken into consideration during the procedure described in Section 2.

Author Contributions: Conceptualization—methodology, P.K.P., I.F.G. and I.A.S.; validation—software, P.K.P. and E.A.P.; writing—review and editing, P.K.P., E.A.P., I.F.G. and I.A.S.; supervision, I.F.G. and I.A.S.; project administration I.A.S. All authors have read and agreed to the published version of the manuscript.

Funding: This research received no external funding.

Data Availability Statement: The data presented in this study are available on request from the corresponding author.

Conflicts of Interest: The authors declare no conflict of interest.

References

1. Joint HBM Working Group ESD Association and JEDEC Solid State Technology Association. User Guide of ANSI/ESDA/JEDEC JS-001 Human Body Model Testing of Integrated Circuits. Available online: https://www.jedec.org/sites/default/files/JTR001-01-12%20Final.pdf (accessed on 8 February 2021).
2. ESD Association. Fundamentals of Electrostatic Discharge Part Five–Device Sensitivity and Testing. Available online: https://www.esda.org/assets/Documents/7dd436d0a3/FundamentalsPart5.pdf (accessed on 9 February 2021).
3. ESD. *Association Standard Test Method. ANSI/ESD STM5.2-2012: Electrostatic Discharge Sensitivity Testing—Machine Model (MM)—Component Level*; Electrostatic Discharge Association (ESD): Rome, NY, USA, 2012.
4. IEC 61000-4-2. Electromagnetic Compatibility (EMC)—Part 4-2: Electrostatic Discharge Immunity Test, ed. 2.0. 2008. Available online: https://webstore.iec.ch/publication/4189 (accessed on 12 February 2021).
5. Hirata, M.; Takahashi, T.; Schibuya, N. Evaluation of Falling Time Restriction of ESD Immunity Test Current Waveform: The Result of IEC 61000-4-2 Round Robin Test in Japan. In Proceedings of the IEEE International Symposium on Electromagnetic Compatibility, Honolulu, HI, USA, 8–13 July 2007; pp. 1–4.
6. Koo, J.; Cai, Q.; Pommerenke, D.; Wang, K.; Mass, J.; Hirata, M.; Martwick, A. The repeatability of system level ESD test and relevant ESD generator parameters. In Proceedings of the IEEE International Symposium on Electromagnetic Compatibility, Detroit, MI, USA, 18–22 August 2008; pp. 1–6.
7. Marathe, S.; Meiguni, J.; Zhou, K.; Pommerenke, D.; Hertz, M. ESD Generator Tip Current Reconstruction Using a Current Probe Measurement at the Ground Strap. In Proceedings of the IEEE International Symposium on Electromagnetic Compatibility, Signal & Power Integrity (EMC+SIPI), New Orleans, LA, USA, 22–26 July 2019; pp. 141–146.
8. Yang, S.; Zhou, J.; Pommerenke, D.; Liu, D. A simple frequency response compensation method for current probe measurements of ESD currents. In Proceedings of the IEEE International Symposium on Electromagnetic Compatibility & Signal/Power Integrity (EMCSI), Washington, DC, USA, 7–11 August 2017; pp. 158–163.
9. Smith, D.C. Current probes, more useful than you think. In Proceedings of the IEEE EMC Symposium. International Symposium on Electromagnetic Compatibility. Symposium Record (Cat. No.98CH36253), Denver, CO, USA, 24–28 August 1998; Volume 1, pp. 284–289.
10. ESD Pulse Calibration Set—Teseq MD 103. Available online: https://www.teseq.com/products/downloads/datasheet/MD_103.pdf (accessed on 12 February 2021).
11. Baran, J.; Sroka, J. Distortion of ESD Generator Pulse Due to Limited Bandwidth of Verification Path. *IEEE Trans. Electromagn. Compat.* **2010**, *52*, 797–803. [CrossRef]
12. Digital Phosphor Oscilloscope—Tektronix TDS7254B. Available online: http://www.testequipmenthq.com/datasheets/TEKTRONIX-TDS7254B-Datasheet.pdf (accessed on 15 February 2021).
13. AC Current Probes—Tektronix CT1-CT2-CT6. Available online: https://www.tek.com/datasheet/current-probe/ct1-ct2-ct6 (accessed on 15 February 2021).
14. Current Monitor Probe—Fischer Custom Communications F-65. Available online: http://www.fischercc.com/products/f-65/ (accessed on 16 February 2021).
15. ESD Generator—EM Test Dito ESD Simulator. Available online: http://www.emtest.com/products/product/13512010000001018 3.php (accessed on 18 February 2021).
16. *ESD Generator—Schaffner NSG 433, ESD Simulator. User Manual*; Teseq: Rocklin, CA, USA, 2012.
17. ESD Generator—Schaffner NSG 438, ESD Simulator. Available online: https://www.teseq.com/products/downloads/datasheet/NSG_438.pdf (accessed on 18 February 2021).
18. *EMC Partner Transient 3000, User Manual*; EMC Partner: Laufen, Switzerland, 2013.
19. Papastamatis, P.K.; Paliatsos, E.A.; Gonos, I.F.; Stathopulos, I.A. Investigation of the Frequency Response Compensation Method for ESD Current Reconstruction for Different Test Levels and ESD Test Generators. In Proceeding of the International Symposium on Electromagnetic Compatibility-EMC EUROPE, Virtual Conference, Rome, Italy, 23–25 September 2020.

20. Carobbi, C.F.M.; Millanta, L.M. Circuit loading in radio-frequency current measurements: The insertion impedance of the transformer probes. *IEEE Trans. Instrum. Meas.* **2010**, *59*, 200–204. [CrossRef]
21. Millanta, L.M. Fundamentals of the EMC Current Probes. In Proceedings of the 12th International Zurich Symposium and Technical Exhibition on Electromagnetic Compatibility, Zürich, Switzerland, 18–20 February 1997; pp. 585–590.
22. Katsivelis, P.K.; Fotis, G.P.; Gonos, I.F.; Koussiouris, T.G.; Stathopulos, I.A. Electrostatic discharge current linear approach and circuit design method. *Energies* **2010**, *3*, 1728–1740. [CrossRef]
23. Vita, V.; Fotis, G.P.; Ekonomou, L. An optimization algorithm for the calculation of the electrostatic discharge current equations' parameters. *WSEAS Trans. Circuits Syst.* **2016**, *15*, 224–228.
24. Caniggia, S.; Maradei, F. Circuit and numerical modeling of electrostatic discharge generators. *IEEE Trans. Ind Appl.* **2006**, *42*, 1350–1357. [CrossRef]
25. Vita, V.C.; Fotis, G.P.; Ekonomou, L. Parameters' optimisation methods for the electrostatic discharge current equation. *Int. J. Energy* **2017**, *11*, 1–6.
26. Takada, T.; Sekine, T.; Asai, H. Circuit/Electromagnetic Hybrid Simulation of Electrostatic Discharge in Contact Discharge Mode. In Proceedings of the International Symposium on Electromagnetic Compatibility—EMC EUROPE, Rome, Italy, 17–21 September 2012; pp. 1–6.
27. Zhou, Y.; Hajjar, J.J. A Circuit Model of Electrostatic Discharge Generators for ESD and EMC SPICE Simulation. In Proceedings of the IEEE International Conference on Electron Devices and Solid-State Circuits, Chengdu, China, 18–20 June 2014; pp. 1–2.
28. Yoshida, T.; Masui, N. A Study on System Level ESD Stress Simulation using Circuit Simulator. In Proceedings of the Asia-Pacific Symposium on Electromagnetic Compatibility (APEMC), Melbourne, Australia, 20–23 May 2013; pp. 1–4.
29. Yousaf, J.; Park, M.; Lee, H.; Youn, J.; Lee, D.; Hwang, C.; Nah, W. Efficient Circuit and an EM Model of an Electrostatic Discharge Generator. *IEEE Trans. Electromagn. Compat.* **2018**, *60*, 1078–1086. [CrossRef]
30. Li, D.Z.; Marathe, S.; Wei, P.; Hosseinbeig, A.; Pommerenke, D. Full-Wave Simulation of System-Level Disruption During Secondary ESD Events in a Smartphone. *IEEE Trans. Electromagn. Compat.* **2019**, *61*, 40–47. [CrossRef]
31. Javor, V.; Lundengård, K.; Rančić, M.; Silvestrov, S. A Study on Frequency Spectrum of Electrostatic Discharge Currents and Lightning Currents. In Proceedings of the 14th International Conference on Advanced Technologies, Systems and Services in Telecommunications (TELSIKS), Nis, Serbia, 23–25 October 2019; pp. 198–201.